

# Aminated glycidyl methacrylates as a support media for goethite nanoparticle enabled hybrid sorbents for arsenic removal: From copolymer synthesis to full-scale system modeling

Khaled Taleb <sup>a</sup>, Jasmina Markovski <sup>b,c,\*</sup>, Kiril D. Hristovski <sup>c</sup>, Vladana N. Rajaković-Ognjanović <sup>d</sup>, Antonije Onjia <sup>b</sup>, Aleksandar Marinković <sup>a</sup>

<sup>a</sup> Faculty of Technology and Metallurgy, University of Belgrade, Karnegijeva 4, 11120 Belgrade, Serbia

<sup>b</sup> Vinča Institute, University of Belgrade, PO Box 522, 11000 Belgrade, Serbia

<sup>c</sup> The Polytechnic School, Ira A. Fulton Schools of Engineering, Arizona State University, 7171 E. Sonoran Arroyo Mall, Mesa, AZ 85212, USA

<sup>d</sup> Faculty of Civil Engineering, University of Belgrade, Bulevar kralja Aleksandra 73, 11000 Belgrade, Serbia

Received 28 January 2016; received in revised form 22 March 2016; accepted 11 April 2016

Available online 11 May 2016

## Abstract

To achieve short mass transfer zones that enable arsenic removal under high hydraulic loading rates and short empty bed contact times needed for small point-of-use packed bed applications, hybrid media was developed and tested. Cross-linked macroporous glycidyl methacrylate copolymer support media was synthesized, amino modified and in-situ impregnated by goethite nanoparticles via an oxidative deposition in a hydrophilic/hydrophobic (water/xylene) system. The media properties were characterized via scanning electron microscopy (SEM), energy dispersive X-ray analysis (EDS), X-ray diffraction (XRD), and surface area analysis. Arsenic removal capabilities of the hybrid goethite impregnated media were evaluated by conducting batch sorption tests, developing isotherms and simulating the breakthrough curve with a pore surface diffusion model (PSDM), after being verified by a short bed column (SBC) test. The high porous media ( $\epsilon_p \approx 0.7$ ) contained ~16% of iron and exhibited Freundlich adsorption capacity parameter of  $K \approx 369 (\mu\text{g g}^{-1})(\text{L } \mu\text{g}^{-1})^{1/n}$  and Freundlich intensity parameter of  $1/n \approx 0.54$ . Without engaging in taxing pilot scale testing, the PSDM was able to provide a good prediction of the media's capacity and intraparticle mass transport properties under high hydraulic loading rates.

© 2016 Tomsk Polytechnic University. Production and hosting by Elsevier B.V. This is an open access article under the CC BY-NC-ND license (<http://creativecommons.org/licenses/by-nc-nd/4.0/>). Peer review under responsibility of Tomsk Polytechnic University.

**Keywords:** Arsenic; Polymer; Goethite; Modeling

## 1. Introduction

Stemming from their rapid population growth, economic development, and climate change, many developing and developed countries are concerned with increasing demands for potable water [1,2]. Although available, potable water is often contaminated with a number of contaminants that prevent its direct use without any treatment [3]. Many of these contaminants are present in an inorganic form in the potable water

sources, and disinfection, granular activated carbon or other inexpensive small system water treatment technologies are not capable of removing them to innocuous level [1,4]. Since the inorganic substances are the major chemical contaminants of potable water, its adverse effects to human populations are of growing concern [5]. For example, more than 70 countries contain high levels of arsenic and endanger lives of several hundred million people [1]. Considering its potential carcinogenicity and toxicity health risks, WHO and US EPA promulgated  $10 \mu\text{g L}^{-1}$  as a maximum contaminant level (MCL) of arsenic in a drinking water [6–8]. Latest toxicological research, however, suggests that the MCL should be further lowered to address the newest acceptable health risks associated with arsenic in drinking water [9]. Consequently, this new regulatory and scientific pressure creates a drive to develop novel technologies capable of addressing the low arsenic MCL challenge.

\* Corresponding author. The Polytechnic School, Ira A. Fulton Schools of Engineering, Arizona State University, 7171 E. Sonoran Arroyo Mall, Mesa, AZ 85212, USA. Tel.: +1 (480) 727 1617; fax: +1 (480) 727 1549.

E-mail address: [jmarkov2@asu.edu](mailto:jmarkov2@asu.edu) (J. Markovski).

Nanomaterials, which could be tailored to exhibit large specific surface area and specific functionality, offer a promise that could help resolve some of the challenges associated with novel small systems arsenic treatment technologies [10–12]. Such systems are probably the only viable water treatment approach capable of addressing the needs of many small communities, which do not have the technological expertise, resources, or infrastructure to employ conventional and energy intensive water treatment systems [3,13]. In the past 15 years, there has been a growing interest in harvesting the unique properties of metal (hydr)oxide nanomaterials for developing adsorptive arsenic treatment technologies, considering that adsorption has been identified as one of the Best Available Technologies (BAT) for small systems' arsenic treatment [4,10,11,14–16]. Nano iron (hydr)oxides, like goethite ( $\alpha$ -FeOOH), have been identified as one of the best candidates for developing nanomaterial based small arsenic treatment systems because of simple fabrication, low cost, high adsorption capacity and selectivity, and thermodynamic stability in naturally fluctuating water matrices [17–20].

When developing small systems for arsenic treatment, it is imperative to ensure simultaneous operational and technological simplicity and efficient performance on a large system scale. These technological targets are difficult to achieve with sorbent technologies that employ suspended nanomaterial reactors because nanomaterials would have to be removed from the treated water before the water is used [21]. This, of course, would necessitate employment of energy intensive membrane filtration technologies, which have their own set of operational challenges [22]. In contrast, fixed bed reactor configurations eliminate these operational challenges, but necessitate the use of either aggregated nanomaterial adsorbents or media composed of nanomaterial sorbent fixed to a macroscopic support platform i.e. hybrid media [10,15,21,23–27]. Aggregation of nanomaterials, especially iron (hydr)oxide based ones, often leads to problems related to adsorbent stability, attrition, surface area decrease, and porosity reduction, which consequently creates operational problems such as head loss, channeling, and nanomaterial release in the treated effluent. Iron (hydr)oxide nanomaterial hybrid sorbents have the potential to minimize these problems with a selection of adequate and mechanically strong and stable support platform. However, to fully utilize the potential offered by iron (hydr)oxide nanomaterials when developing these hybrid media for small treatment systems, the support material has to exhibit high macroporosity, which: (1) minimizes pore clogging during in-situ nanomaterial synthesis; (2) enables fast intraparticle mass transport at high hydraulic loading rates and empty bed contact times (EBCTs); (3) creates short mass transfer zones; and (4) allows for base material functionalization to obtain synergetic properties for simultaneous removal of other contaminants [15,23,25,26,28].

Glycidyl methacrylate based copolymers represent an ideal candidate for development of macroporous base media that fits the abovementioned criteria. These copolymers enable inexpensive controllable production of spherical nanoparticle support media with different geometries, and permits design of

intraparticle properties via a number of versatile ring-opening reactions of the pendant epoxy groups [29]. Furthermore, the fabrication of these base support media could be optimized to maximize porosity while maintaining high mechanical strength and uniformity of the microscopic hybrid media.

The goal of this study was to evaluate the suitability of the developed goethite impregnated cross-linked macroporous copolymer media for removing arsenic from water. To achieve this goal, the following steps were undertaken: (1) fabricate macroporous copolymer support media using suspension polymerization followed by amino modification and in-situ impregnation by goethite nanoparticles; (2) characterize adsorbent media; (3) quantify the adsorption capacity by conducting pseudo-equilibrium tests under model conditions; (4) quantify the mass transport processes that control the rate of arsenic adsorption in a fixed bed column; (5) predict the performance of a full scale system using the pore surface diffusion model (PSDM).

## 2. Experimental and modeling approach

### 2.1. Fabrication of aminated glycidyl methacrylate support media

Macroporous glycidyl methacrylate copolymer was fabricated by dissolving 3.9 g of poly(*N*-vinyl pyrrolidone (PVP Kollidon 90, BASF) in 300 mL of deionized water (18 M $\Omega$  cm), and then mixed with oil phase consisting of monomer precursors, porogen and initiator as it is depicted in Fig. 1. The monomer precursor was composed of 30 mL glycidyl methacrylate (Merck) and 13 mL ethylene glycol dimethacrylate (Fluka), while 20 mL of 2-hexanone (Merck) was used as a porogen agent, and 1 g of 2,2'-azobis(2-methyl propionitrile) (Merck) as initiator. The two phases were vigorously stirred under inert atmosphere of nitrogen at 80 °C for a period of 2 h to facilitate a suspension polymerization process. The created copolymer was separated by filtration, washed firstly with ethanol (Sigma Aldrich) followed by deionized water, aged in ethanol for a period of 12 h, and then dried in a vacuum oven at 40 °C for 4 h. The porogen agent was removed from the copolymer by a 48 h continuous Soxhlet extraction with chloroform (Sigma Aldrich). The obtained material was sieved and material consisted from the fraction in a range 150–600  $\mu$ m was collected, and used in subsequent experiments.

Upon sieving, 10 g of glycidyl methacrylate copolymer was dispersed in 50 mL of dry tetrahydrofuran (Sigma Aldrich), and then 20 mL of diethylene triamine (Merck) was added drop-wise to initiate the amination reaction, which was conducted at 60 °C for a period of 6 h as it illustrated in Fig. 1. Introduction of terminal amino groups was conducted to demonstrate the possibility of functionalizing this base media and utilize the affinity of terminal amino groups to facilitate iron precursor diffusion. Modification of copolymer enriched by hydrophilic amino group helped surface wetting and more importantly the interaction of Lewis acid (ferric ions) with Lewis base site (surface amino groups) provides initial nucleation center for goethite precipitation. The aminated macroporous glycidyl methacrylate support media was then

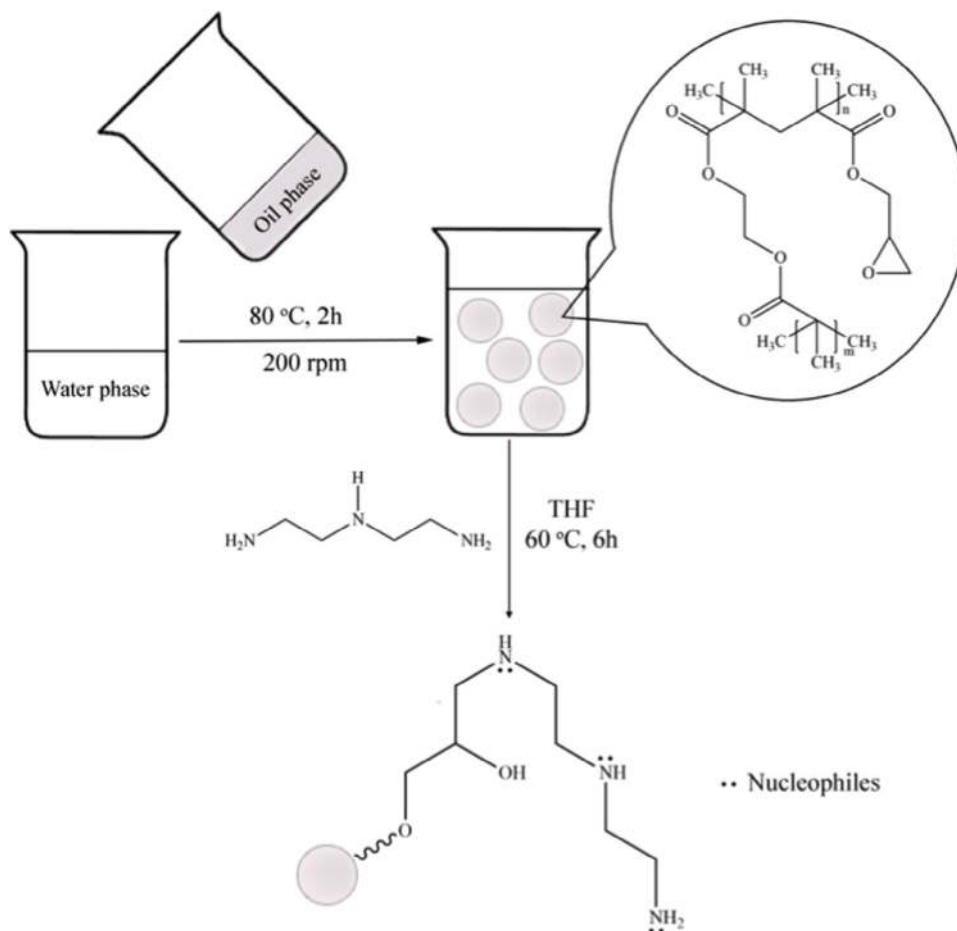


Fig. 1. Schematic view of the steps applied for fabrication of the aminated glycidyl methacrylate support media.

filtered, washed with ethanol and deionized water, collected, and dried in a vacuum oven at 40 °C for 6 hours.

## 2.2. Controllable impregnation of the support media with goethite

In order to increase the effectiveness of iron transport inside hydrophilic support media, mixture of hydrophilic (water)/hydrophobic (xylene) (Merck) solvents was applied. A 10 g of the aminated glycidyl methacrylate copolymer was soaked with xylene and placed in a perforated column assembly as illustrated in Fig. 2. Xylene was used as a copolymer suspension system, which was mixed by nitrogen bubbling throughout the reactor in an upstream flow to provide a gentle movement/mixing of packed copolymer. Upon establishing a steady mixing and continuous flow of nitrogen ( $15 \text{ mL min}^{-1}$ ) through two phase system xylene/copolymer, 30 mL of  $\text{FeCl}_2 \times 4\text{H}_2\text{O}$  (Merck) ( $0.5 \text{ mol L}^{-1}$ ) aqueous solution was added in the reactor over a 15 min period via a dropping funnel located at the top of reactor column. A glass frit assembly connected to the funnel was used to provide for homogeneous dispersion of  $\text{FeCl}_2$ /water droplets. Small droplets of the  $\text{FeCl}_2$ /water solution were attracted by hydrophilic copolymer, and nitrogen bubbling promotes formation of uniform film at surface and increase the effectiveness of iron transport inside the copolymer. After additional bubbling of  $\text{N}_2$  for 15 min, precipitation of goethite was

performed in air at  $\text{pH } 7 \pm 0.2$  by neutralizing the generated acid with  $1 \text{ mol L}^{-1}$   $\text{NaHCO}_3$  (Zorka Pharma) buffer solution [19]. Bubbling of air was continued for a period of 24 h to complete the oxidation of the ferrous ions to ferric, and ensure

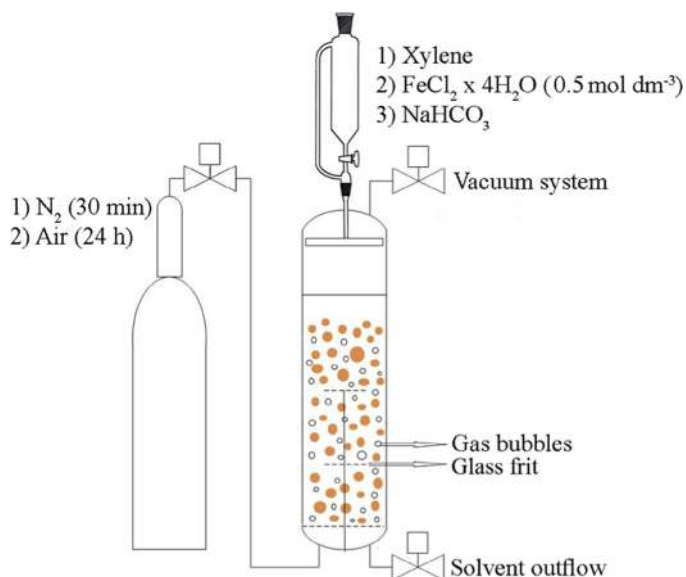


Fig. 2. Schematics of the copolymer impregnation assembly.

complete formation of goethite. The change of the green–blue color to an ochreous shade of precipitated material was an indicator of completed oxidation/precipitation process.

The first step of impregnation is completed by exhaustion of the column (removal of liquid phase), followed by careful vacuum drying. The entire media impregnation with iron was repeated. The newly fabricated goethite impregnated media was then washed with deionized water, filtrated and dried at 40 °C for 10 h, and further characterized.

### 2.3. Media characterization

Media morphology was analyzed by scanning electron microscopy (FEG–SEM) (TESCAN MIRA3). An average diameter of adsorbents was determined using MIRA TESCAN in-situ measurement software. Energy dispersion X-ray analysis (EDS) (INCAEnergy 350 Microanalysis System) method was used for determination of elemental content of goethite impregnated media. The structural analysis of goethite impregnated media was performed using X-ray diffraction (XRD) (BRUKER D8 ADVANCE). The specific surface area and average pore volume were estimated using Micromeritics ASAP 2020 surface area analyzer. The textural parameters were calculated by using the BET (Brunauer–Emmett–Teller) and BJH (Barrett–Joyner–Halenda) method. Adsorbent media density and porosity were evaluated by pycnometer analysis according to procedure presented by the Sontheimer et al. (1988) [30]. Assuming cylindrical pores, the average pore diameter was calculated from the surface area–pore volume ratio [10,24,31] (Eq. 1):

$$\frac{2}{r_{\text{pore}}} = \frac{A_{\text{ad}}}{V_{\text{ad}}} \quad (1)$$

where  $r_{\text{pore}}$  is the average pore radius (m);  $A_{\text{ad}}$  is the surface area of the adsorbent ( $\text{m}^2$ ); and  $V_{\text{ad}}$  is the pore volume of the adsorbent ( $\text{m}^3$ ).

Quantification of epoxy and amino groups were performed according to the literature volumetric methods [32,33]. The pH values at the point of zero charge (pHpzc) of goethite impregnated media were measured using the pH drift method [34]. In brief, 0.50 g of goethite impregnated media was added to 50 mL of  $\text{KNO}_3$  solution ( $0.1 \text{ mol L}^{-1}$ ). The initial pH values of samples were in the range from 2 to 11 and were adjusted by adding a small amount of HCl or NaOH solution with concentration of  $0.1 \text{ mol L}^{-1}$ . The samples were shaken for 3 days at room temperature of  $22 \pm 2 \text{ }^\circ\text{C}$ .

### 2.4. Equilibrium adsorption experiments

Arsenic removal in batch adsorption experiments with goethite impregnated media was conducted in 10 mL arsenic-only water with initial arsenic concentration  $C_0$  ( $\text{As}$ )  $\approx 100 \text{ } \mu\text{g L}^{-1}$  with adsorbent dosages of 100–500  $\text{mg L}^{-1}$  at pH value of  $6.7 \pm 0.2$ . Although natural waters typically exhibit pH between 6.5 and 8.5, lower end pH values were used to ensure better experimental sensitivity stemming from higher arsenic capacity of goethite at lower pH values. The sample solutions were agitated for 1 day to ensure complete pseudo-

equilibrium. Prior to the analysis, adsorbent was removed from the suspension by the filtration through a Millipore 0.22  $\mu\text{m}$  membrane filter (Bedford, MA, USA). Adsorption equilibrium was analyzed using the Freundlich adsorption isotherm model (Eq. (2)).

$$q = K \times C_e^{1/n} \quad (2)$$

where  $q$  is adsorption capacity ( $\mu\text{g g}^{-1}$ ),  $C_e$  is the equilibrium concentration of adsorbate in solution ( $\mu\text{g L}^{-1}$ ),  $K$  is the Freundlich adsorption capacity parameter ( $\mu\text{g g}^{-1}(\text{L } \mu\text{g}^{-1})^{1/n}$ ), and  $1/n$  is the unitless Freundlich adsorption intensity parameter.

Arsenic concentrations in solution after adsorption experiments were analyzed by the use of inductively coupled plasma mass spectrometry (ICP-MS), using an Agilent 7500ce ICP-MS system (Waldbronn, Germany).

### 2.5. Pore Surface Diffusion Model prediction of a short bed column performance and its verification via a Short Bed Column Test

Arsenic breakthrough curve of short bed column (SBC) was predicted by the Pore Surface Diffusion Model (PSDM) using the AdDesignS<sup>TM</sup> software developed by Michigan Technological University [35]. PSDM is a dynamic packed bed model that covers both pore and surface diffusion models and has been successfully applied in the prediction of the breakthrough curve and the feasibility of adsorbent media [10,24,26,36–40].

Determination of the external mass transport coefficient were based on the Gnielinski correlation [30]:

$$k_f = \frac{[1 + 1.5(1 - e)] \times D_l}{d_p} \times (2 + 0.644 \times Re^{1/2} \times Sc^{1/3}) \quad (3)$$

$$Re = \frac{\rho_l \times \Phi \times d_p \times v_l}{e \times \mu_l} \quad (4)$$

$$Sc = \frac{\mu_l}{\rho_l \times D_l} \quad (5)$$

Constraints:  $Re \times Sc > 500$ ;  $0.6 \leq Sc \leq 10^4$ ;  $1 \leq Re \leq 100$ ;  $0.26 \leq e \leq 0.935$ ;  $k_f$  is the external mass transport coefficient (calculated  $k_f \approx 6.5 \times 10^{-3} \text{ cm s}^{-1}$ );  $Re$  is the Reynolds number (unitless);  $Sc$  is the Schmidt number (unitless);  $d_p$  is the adsorbent particle diameter ( $d_p = 0.30 \times 10^{-3} \text{ m}$ );  $D_l$  is the free liquid diffusivity for arsenate ( $D_l = 9.05 \times 10^{-10} \text{ m}^2 \text{ s}^{-1}$ );  $e$  is the bed void fraction ( $e = 0.4$ );  $\mu_l$  is the dynamic viscosity of water at 20 °C ( $\mu_l = 1.002 \times 10^{-3} \text{ N s m}^{-2}$ );  $\rho_l$  is the density of water at 20 °C ( $\rho_l = 998.2 \text{ kg m}^{-3}$ );  $\Phi$  is the particle shape factor ( $\Phi = 1$ );  $v_l$  is the liquid superficial velocity ( $v_l \approx 0.00265 \text{ m s}^{-1}$ ).

Considering that the material was very porous (the particle porosity  $e_p \approx 0.7$ ), the impact of surface diffusion was assumed negligible and the pore diffusion coefficient was estimated using Eq. (6) [10,24,26,30,39,41]:

$$D_p = \frac{e_p \times D_l}{\tau} \quad (6)$$



Applying the correlation for electrolyte solutions (Eq. (7)), the tortuosity was determined [10,24,26,39,42]:

$$\tau = \frac{(2 - e_p)^2}{e_p} \quad (7)$$

The estimated value for tortuosity and the pore diffusion coefficient were  $\tau \approx 2.4$  and  $D_p \approx 2.6 \times 10^{-6} \text{ cm}^2 \text{ s}^{-1}$ , respectively.

The relative importance of internal and external mass transport resistance was evaluated by estimating the pore ( $Bi_p$ ) Biot numbers using the relationship given by Eq. (8) [10,24,26,39]:

$$Bi_p = \frac{k_f \times d_p}{2 \times D_p} \quad (8)$$

Although a number of studies have verified the validity of the PSDM to predict breakthrough curves of arsenic-only water matrices [10,24,26,39,43], the SBC tests were conducted under the same pH and arsenic concentration conditions in order to validate PSDM prediction of arsenic removal by hybrid media.

In the SBC test, 0.4 g of goethite impregnated media was packed atop a support of cotton and glass beads were placed above and below to provide evenly distributed flow. Wall effect on the mass transfer was neglected since used adsorbent media provided  $d_{\text{column}}/d_p$  ratio of  $\sim 40$  [44]. Arsenic-only water with initial arsenic concentration of  $\sim 150 \mu\text{g L}^{-1}$  was introduced through the column until complete breakthrough ( $C_e/C_o > 95\%$ ) at hydraulic loading rate of  $2.65 \text{ L m}^{-2} \text{ s}^{-1}$  ( $4.2 \text{ gpm ft}^{-2}$ ), which is within the recommended loading rates for full scale operations [45]. Although relatively high, this hydraulic loading rate was adequate in capturing the mass transfer zone and minimizing the film mass transport limitation.

### 2.6. Full-scale system modeling using validated pore surface diffusion model

The validated PSDM was used to model the performance of full-scale fix bed systems operating at the same loading rate as the SBC tests. The length of the packed bed was changed to achieve the desired EBCTs of 2.5, 5, and 10 min. The modeling was conducted with a realistic value of arsenic  $C_o = 30 \mu\text{g L}^{-1}$  while the water chemistry, pH, and bed porosity were assumed to be the same as those used in the SBC test [10,24].

## 3. Results and discussion

### 3.1. Media characterization

Fig. 3 illustrates the aminated macroporous glycidyl methacrylate copolymer before and after impregnation with goethite nanoparticles. As depicted in Fig. 3a, the media was characterized by spherical particles ranging between 150 and 600  $\mu\text{m}$  in size, with an average diameter of 300  $\mu\text{m}$ . The media exhibited large pores that were uniformly distributed on the surface and through the media (Fig. 3b and c). The presence of the goethite nanoparticles inside the pores of the media in a manner that creates a nanostructured protuberances and cavities is illustrated in Fig. 3d.

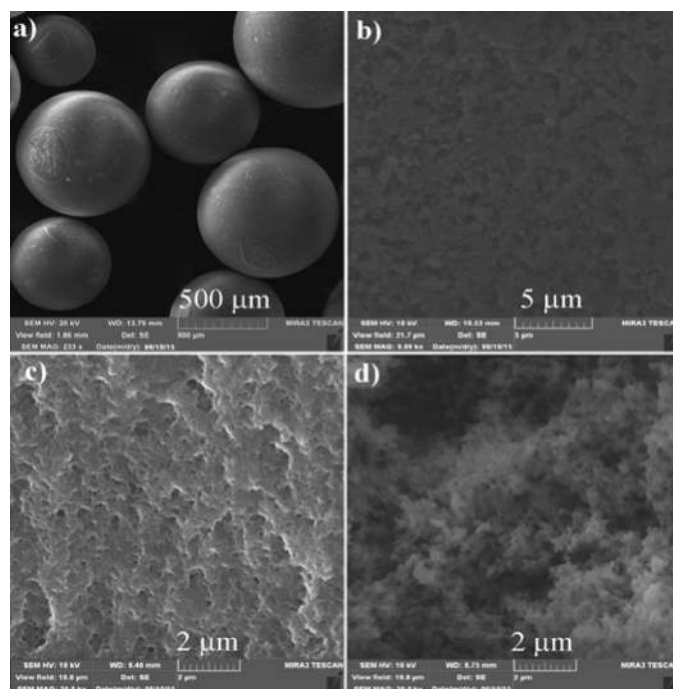


Fig. 3. Aminated macroporous glycidyl methacrylate copolymer (a) spheres, (b) surface, (c) cross-section of virgin media, and (d) cross-section of goethite impregnated media.

The results of pore and surface area analysis of the goethite impregnated media showed an estimated specific surface area of  $43 \text{ m}^2 \text{ g}^{-1}$ . The average pore diameter and an average specific pore volume were estimated at 85 nm and  $1.44 \text{ cm}^3 \text{ g}^{-1}$ , respectively, which confirmed the macroporous nature of this media. Equation (1) provided a more conservative estimate of the average pore diameter. Assuming cylindrical pores, the average pore diameter was 67 nm, which is slightly lower than  $\text{N}_2$  pore analysis results, but still in accordance with definition of IUPAC limit for macroporous materials of  $>50 \text{ nm}$  [46].

The gravimetric analysis showed that the impregnated media contained  $\sim 16\%$  of iron which was in compliance with EDS analyses illustrated in Fig. 4. According to EDS analyses, iron was relatively evenly distributed throughout the outer layers which exhibited slightly higher Fe content (21.5%) than the center (15.8%). Observed higher iron content on sphere surface is expected due to more favorable mass transfer compared to center. High iron content and uniform distribution at overall media surface confirms that established procedure for amino modification and goethite impregnation of glycidyl methacrylate copolymer is optimized. The high content of both epoxy and amino groups,  $3.2 \text{ mmol g}^{-1}$  and  $6.9 \text{ mmol g}^{-1}$ , respectively, further supported the conjecture that this media could be easily functionalized to develop sites capable of removing contaminants with chemistries different than arsenic.

Fig. 5 confirms presence of goethite. The XRD spectra of the goethite impregnated media show characteristic peaks observed at the  $2\theta$  values of 17.8, 21.2, 33.2, 36.6 and  $53.2^\circ$ , corresponding to goethite structure (ICDD PDF2 No. 81-0464). Three factors may be the reason of the obtained

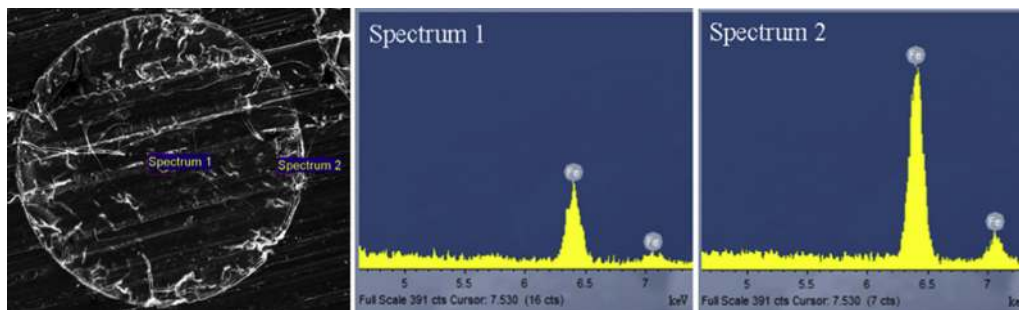


Fig. 4. EDS analysis of goethite impregnated media at central and outer point.

significant XRD peak broadening: (1) the influence of polymer support; (2) amorphous phase of goethite and (3) small size of goethite particles.

### 3.2. Removal of arsenic under pseudo-equilibrium batch conditions

Fig. 6 presents the Freundlich arsenic adsorption isotherm in arsenic-only water which is characterized by a Freundlich adsorption capacity parameter of  $K \approx 369 (\mu\text{g g}^{-1})(\text{L } \mu\text{g}^{-1})^{1/n}$  and Freundlich intensity parameter of  $1/n \approx 0.54$ . Obtained  $K$  value is in the range of reported values for nanostructured  $\text{ZrO}_2$  spheres [24], however, in comparison to activated carbon and ion-exchange resin modified with nano-iron (hydr)oxide [15,47], goethite impregnated media exhibits higher adsorption capacity. Since point of zero charge of the goethite impregnated media was estimated at  $\text{pH}_{\text{PZC}} \approx 7.7$ , the favorable adsorption process under the experimental thermodynamic conditions ( $1/n < 1$ ) stems from the positively charged surface of the media and the negatively charged arsenate species ( $\text{H}_2\text{AsO}_4^-$  and  $\text{HAsO}_4^{2-}$ ), which are dominant at pH range of the conducted sorption experiments [48–51].

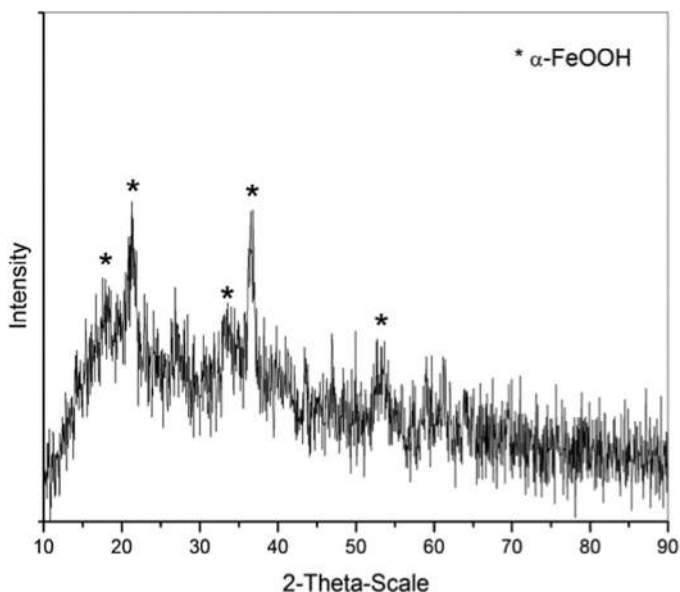


Fig. 5. XRD analysis of the goethite impregnated media.

### 3.3. Short bed adsorbent test and pore surface diffusion modeling

The PSDM prediction and experimental data from the SBC tests are presented in Fig. 7. For the initially estimated  $k_f \approx 6.5 \times 10^{-3} \text{ cm s}^{-1}$  and  $D_p \approx 2.6 \times 10^{-6} \text{ cm}^2 \text{ s}^{-1}$ , the PSDM provided a good prediction ( $R^2 = 0.93$ ). Considering high porosity of the material (the particle porosity  $\epsilon_p \approx 0.7$ ) and strong inner-sphere complexes that arsenic forms with goethite via oxygen bridges, it is verified that surface diffusion can be ignored in comparison to several orders of magnitude higher pore diffusion [52–56].

The estimated Biot number ( $\text{Bi}_p$ ) was 43 and confirmed that the intraparticle diffusion controls the overall mass transport [41]. As illustrated, breakthrough occurred rapidly for  $C/C_o \approx 0.5$  at 2500 BVT and for  $C/C_o \approx 0.95$  at 66 000 BVT.

### 3.4. Performance of full-scale packed bed systems

In order to evaluate the suitability of the developed goethite impregnated media for removing arsenic from water, the performance of a full scale system is predicted by the use of validated pore surface diffusion model at commonly used EBCTs. As illustrated in Fig. 8, the number of bed volumes that can be treated until the maximum contaminant level (MCL) of  $10 \mu\text{g L}^{-1}$  is directly related to EBCT. The PSDM predicted that for  $C/C_o \approx 0.33$ , 26 000 bed volumes can be treated at EBCT of

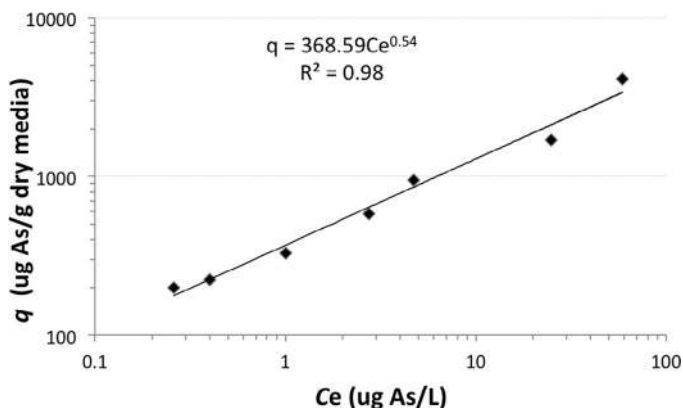


Fig. 6. Arsenic adsorption isotherms for goethite impregnated media in arsenic-only water after a contact time of 1 day at 20 °C ( $C_o(\text{As}) \approx 100 \mu\text{g L}^{-1}$ ,  $\text{pH } 6.7 \pm 0.2$ ).

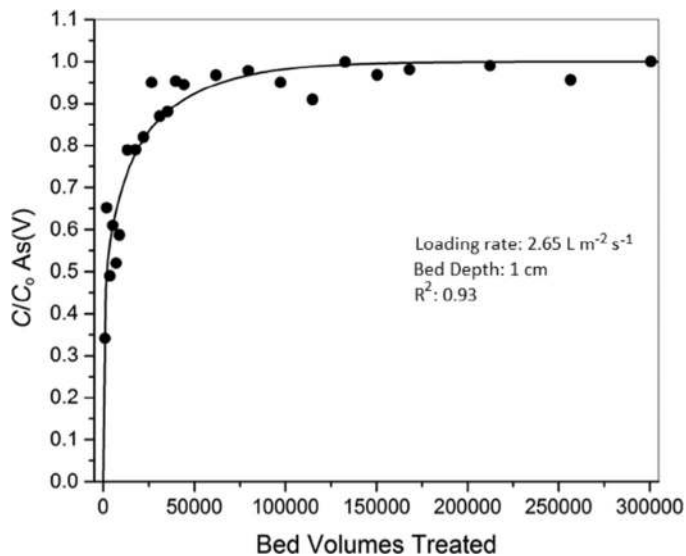


Fig. 7. PSDM prediction and experimental data from the SBA tests for goethite impregnated media in arsenic-only water at 20 °C ( $C_0(\text{As}) \approx 150 \mu\text{g L}^{-1}$ , pH  $6.7 \pm 0.2$ ).

2.5 min. This number increases to 27 000 and 28 000 with increase of the EBCT to 5 and 10 min, respectively, implying that more bed volumes can be treated by extending the EBCT.

#### 4. Conclusions

This study demonstrated that glycidyl methacrylate copolymer exhibits high macroporosity which enables fast intraparticle mass transport at high hydraulic loading rates and creates short mass transfer zones in fixed bed reactor configuration. Amination of pendant epoxy groups of macroporous glycidyl methacrylate support facilitated fabrication of hybrid media applicable in small treatment systems. By selecting the appropriate solvent mixture, goethite impregnation on the

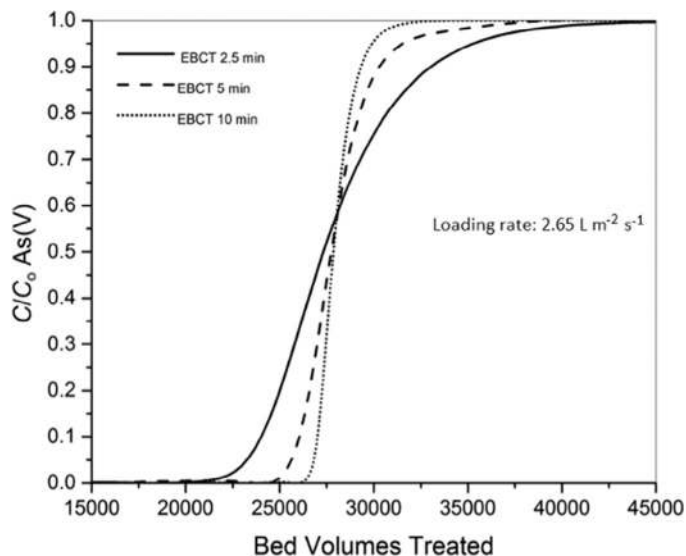


Fig. 8. PSDM prediction of a full-scale system packed with goethite impregnated media in arsenic-only water at 20 °C ( $C_0(\text{As}) \approx 30 \mu\text{g L}^{-1}$ , pH  $6.7 \pm 0.2$ ).

surface and inside the pores of aminated glycidyl methacrylate support media has been achieved uniformly while pore clogging during in-situ nanomaterial synthesis was minimized. Designed goethite impregnated media showed to be effective in a simple water matrix without competition ions and applied methodology of PSDM full-scale packed bed simulation operated under realistic conditions showed to be reliable and significantly simpler than time-consuming and expensive pilot tests. Furthermore, the high content of epoxy groups in stable macroporous support enable functionalization with quaternary amine and create opportunities of development media capable of simultaneous removal of multiple contaminants with chemistries different than arsenic.

#### Acknowledgments

The study was supported in part with funds from Ministry of Education, Science and Technological Development of the Republic of Serbia, (Project No. III43009).

#### References

- [1] P. Ravenscroft, H. Brammer, K. Richards (Eds.), *Arsenic Pollution: A Global Synthesis*, John Wiley & Sons, United Kingdom, 2009.
- [2] J.J. Bogardi, D. Dudgeon, R. Lawford, E. Flinkerbusch, A. Meyn, C. Pahl-Wost, et al., *Water security for a planet under pressure: interconnected challenges of a changing world call for sustainable solutions*, *Curr. Opin. Environ. Sustain.* 4 (2012) 35–43.
- [3] P.A. Berg, *The world's need for household water treatment*, *J. Am. Water Works Assoc.* 107 (10) (2015) 36–44.
- [4] D. Mohan, C.U. Pittman Jr., *Arsenic removal from water/wastewater using adsorbents – a critical review*, *J. Hazard. Mater.* 142 (2007) 1–53.
- [5] J.K. Fawell, *The impact of inorganic chemicals on water quality and health*, *Ann. Ist. Super. Sanita* 29 (2) (1993) 293–303.
- [6] Environmental Protection Agency, *National Primary Drinking Water Regulations; Arsenic and Clarifications to Compliance and New Source Contaminants Monitoring*, Washington, 2001.
- [7] World Health Organization (WHO), *Guidelines for Drinking Water Quality*, vol. 1, third ed., Recommendations, Geneva, Switzerland, 2008.
- [8] World Health Organization (WHO), *Guideline for Drinking-Water Quality*, fourth ed., World Health Organization, Geneva, Switzerland, 2011.
- [9] US Department of Health and Human Services, *Toxicological Profile for Arsenic*, Public Health Service Agency for Toxic Substances and Disease Registry, Atlanta, Georgia, 2007.
- [10] K. Hristovski, P. Westerhoff, J. Crittenden, *An approach for evaluating nanomaterials for use as packed bed adsorber media: a case study of arsenate removal by titanate nanofibers*, *J. Hazard. Mater.* 156 (2008) 604–611.
- [11] M. Hua, S. Zhang, B. Pan, W. Zhang, L. Lv, Q. Zhang, *Heavy metal removal from water/wastewater by nanosized metal oxides: a review*, *J. Hazard. Mater.* 211–212 (2012) 317–331.
- [12] X. Qu, P.J.J. Alvarez, Q. Li, *Applications of nanotechnology in water and wastewater treatment*, *Water Res.* 47 (2013) 3931–3946.
- [13] J.Q. Jiang, *Removing arsenic from groundwater for the developing world – a review*, *Water Sci. Technol.* 44 (2001) 89–98.
- [14] P. Westerhoff, D. Highfield, M. Badruzzaman, Y. Yoon, *Rapid small-scale column tests for arsenate removal in iron oxide packed bed columns*, *J. Environ. Eng. (New York)* 131 (2) (2005) 262–271.
- [15] K.D. Hristovski, P.K. Westerhoff, T. Moller, P. Sylvester, *Effect of synthesis conditions on nano-iron (hydr)oxide impregnated granulated activated carbon*, *Chem. Eng. J.* 146 (2) (2009) 237–243.
- [16] L. Chen, H. Xin, Y. Fang, C. Zhang, F. Zhang, X. Cao, et al., *Application of metal oxide heterostructures in arsenic removal from contaminated water*, *J. Nanomater.* (2014) doi:10.1155/2014/793610.



- [17] S. Fendorf, M.J. Eick, P. Grossl, D.L. Sparks, Arsenate and chromate retention mechanisms on goethite. 1. Surface structure, *Environ. Sci. Technol.* 31 (1997) 315–320.
- [18] P.R. Grossl, M. Eick, D. Sparks, S. Goldberg, C.C. Ainsworth, Arsenate and chromate retention mechanisms on goethite. 2. kinetic evaluation using a pressure-jump relaxation technique, *Environ. Sci. Technol.* 31 (1997) 321–326.
- [19] U. Schwertmann, R.M. Cornell, *Iron Oxides in the Laboratory, Preparation and Characterization*, second ed., Wiley-VCH Verlag GmbH, 2000.
- [20] H. Liu, T. Chen, R.L. Frost, An overview of the role of goethite surfaces in the environment, *Chemosphere* 103 (2014) 1–11.
- [21] J. Trujillo-Reyes, J.R. Peralta-Videa, J.L. Gardea-Torresdey, Supported and unsupported nanomaterials for water and soil remediation: are they a useful solution for worldwide pollution, *J. Hazard. Mater.* 280 (2014) 487–503.
- [22] D.A. Ladner, M. Steele, A. Weir, K. Hristovski, P. Westerhoff, Functionalized nanoparticle interactions with polymeric membranes, *J. Hazard. Mater.* 211–212 (2012) 288–295.
- [23] M.J. DeMarco, A.K. SenGupta, J.E. Greenleaf, Arsenic removal using a polymeric/inorganic hybrid sorbent, *Water Res.* 37 (2003) 164–176.
- [24] K.D. Hristovski, P.K. Westerhoff, J.C. Crittenden, L.W. Olson, Arsenate removal by nanostructured ZrO<sub>2</sub> spheres, *Environ. Sci. Technol.* 42 (2008) 3786–3790.
- [25] S. Sarkar, P.K. Chatterjee, L.H. Cumball, A.K. SenGupta, Hybrid ion exchanger supported nanocomposites: sorption and sensing for environmental applications, *Chem. Eng. J.* 166 (2011) 923–931.
- [26] G. Athanasiaki, L. Sherrill, K.D. Hristovski, The pore surface diffusion model as a tool for rapid screening of novel nanomaterial-enhanced hybrid ion-exchange media, *Environ. Sci.: Water Res. Technol.* 1 (2015) 448–456.
- [27] D. MedPELLI, R. Sandoval, L. Sherrill, K. Hristovski, D.-K. Seo, Iron oxide-modified nanoporous geopolymers for arsenic removal from ground water, *REFFIT*. 1 (2015) 19–27.
- [28] J. Elton, K. Hristovski, P. Westerhoff, Titanium dioxide-based hybrid ion-exchange media for simultaneous removal of arsenic and nitrate, in: S. Ahuja (Ed.), *Novel Solutions to Water Pollution*, American Chemical Society, Washington, 2013, pp. 223–236.
- [29] M.I. Barroso (Ed.), *Reactive and Functional Polymers Research Advances*, Nova Science Publisher Inc., New York, 2008.
- [30] H. Sontheimer, J. Crittenden, S. Summers, *Activated Carbon for Water Treatment*, second ed., DVGW-Forschungsstelle, Engler-Bunte Institut, Universität Karlsruhe, Karlsruhe, Germany, 1988.
- [31] J.C. Crittenden, R.R. Trussell, D.W. Hand, K.J. Howe, G. Tchobanoglous (Eds.), *Water Treatment: Principles and Design*, second ed., Wiley & Sons, Inc., Hoboken, NJ, 2005.
- [32] A.J. Durbetaki, Direct titration of oxirane oxygen with hydrogen bromide in acetic acid, *Anal. Chem.* 28 (1956) 2000–2011.
- [33] H.S. Jung, D.S. Moon, J.K. Lee, Quantitative analysis and efficient surface modification of silica nanoparticles, *J. Nanomater.* (2012) doi:10.1155/2012/593471.
- [34] S.K. Milonjić, L.S. Čerović, Đ.M. Čokeša, S. Zec, The influence of cationic impurities in silica on its crystallization and point of zero charge, *J. Colloid Interface Sci.* 309 (2007) 155–159.
- [35] K.A. Mertz, F. Gobin, D.W. Hand, D.R. Hokanson, J.C. Crittenden, *Manual: Adsorption Design Software for Windows (Ad-DesignS)*, Michigan Technological University, Houghton, Michigan, 1999.
- [36] J.C. Crittenden, N.J. Hutzler, D.G. Geyer, J.L. Oravitz, G. Friedman, Transport of organic compounds with saturated groundwater flow: model development and parameter sensitivity, *Water Resour. Res.* 22 (1986) 271–284.
- [37] D.W. Hand, J.C. Crittenden, D.R. Hokanson, J.L. Bulloch, Predicting the performance of fixed-bed granular activated carbon adsorbers, *Water Sci. Technol.* 35 (7) (1997) 235–241.
- [38] M.L. Magnuson, T.F. Speth, Quantitative structure-property relationships for enhancing predictions of synthetic organic chemical removal from drinking water by granular activated carbon, *Environ. Sci. Technol.* 39 (2005) 7706–7711.
- [39] A.M. Cooper, K.D. Hristovski, T. Möller, P. Westerhoff, P. Sylvester, The effect of carbon type on arsenic and trichloroethylene removal capabilities of iron (hydr)oxide nanoparticle-impregnated granulated activated carbons, *J. Hazard. Mater.* 183 (2010) 381–388.
- [40] D. Yan, D.D. Gang, N. Zhang, L. Lin, Adsorptive selenite removal using iron-coated gac: modeling selenite breakthrough with the pore surface diffusion model, *J. Environ. Eng. (New York)* 139 (2) (2013) 213–219.
- [41] W.I. Weber, H. Sontheimer, J.C. Crittenden, S. Summers, *Activated Carbon for Water Treatment*, second ed., DVGW-Forschungsstelle, Engler-Bunte Institut, Universität Karlsruhe, Karlsruhe, Germany, 1988.
- [42] D.M. LeVan, G. Carta, C.M. Yon, Adsorption and ion exchange, in: R.D. Perry, D.W. Green (Eds.), *Perry's Chemical Engineers' Handbook*, seventh ed., McGraw-Hill, New York, USA, 1997.
- [43] K. Hristovski, P. Westerhoff, T. Möller, P. Sylvester, W. Condit, H. Mash, Simultaneous removal of perchlorate and arsenate by ion-exchange media modified with nanostructured iron (hydr)oxide, *J. Hazard. Mater.* 152 (2008) 397–406.
- [44] E.H. Smith, W.J. Weber, Modeling activated carbon adsorption of target organic-compounds from leachate-contaminated groundwaters, *Environ. Sci. Technol.* 22 (3) (1988) 313–321.
- [45] P.M. Armenante, *Adsorption with Granular Activated Carbon (GAC)*, New Jersey Institute of Technology, 2012.
- [46] K.S.W. Sing, D.H. Everett, R.A.W. Haul, L. Moscou, A. Pierotti, J. Rouquerol, et al., Reporting physisorption data for gas/solid systems with special reference to the determination of surface area and porosity, *Pure Appl. Chem.* 57 (1985) 603–619.
- [47] S. Dale, J. Markovski, K.D. Hristovski, Modeling packed bed sorbent systems with the Pore Surface Diffusion Model: evidence of facilitated surface diffusion of arsenate in nano-metal (hydr)oxide hybrid ion exchange media, *Sci. Total Environ.* (2015) doi:10.1016/j.scitotenv.2015.11.176.
- [48] J.A. Wilkie, J.G. Hering, Adsorption of arsenic onto hydrous ferric oxide: effects of adsorbate-adsorbent ratios and co-occurring solutes, *Colloids Surf. A Physicochem. Eng. Asp.* 107 (1996) 97–110.
- [49] A. Jain, R.H. Loeppert, Effect of competing anions on the adsorption of arsenate and arsenite by ferrihydrite, *J. Environ. Qual.* 29 (2000) 1422–1430.
- [50] X.G. Meng, S.B. Bang, G.P. Korfiatis, Effects of silicate, sulfate, and carbonate on arsenic removal by ferric chloride, *Water Res.* 34 (2000) 1255–1261.
- [51] P.L. Smedley, D.G. Kinniburgh, A review of the source, behaviour and distribution of arsenic in natural waters, *Appl. Geochem.* 17 (2002) 517–568.
- [52] D. Sherman, The electronic structures of Fe<sup>3+</sup> coordination sites in iron oxides; applications to spectra, bonding, and magnetism, *Phys. Chem. Miner.* 12 (1985) 161–175.
- [53] S. Goldberg, C.T. Johnston, Mechanisms of arsenic adsorption on amorphous oxides evaluated using macroscopic measurements, vibrational spectroscopy, and surface complexation modeling, *J. Colloid Interface Sci.* 234 (2001) 204–216.
- [54] B. Manning, S. Fendorf, B. Bostick, D. Suarez, Arsenic(III) oxidation and arsenic(V) adsorption reactions on synthetic birnessite, *Environ. Sci. Technol.* 36 (5) (2002) 976–981.
- [55] D. Sherman, S.R. Randall, Surface complexation of arsenic(V) to iron(III) (hydr)oxides: structural mechanism from ab initio molecular geometries and EXAFS spectroscopy, *Geochim. Cosmochim. Acta* 67 (22) (2003) 4223–4230.
- [56] J. Farrell, B.K. Chaudhary, Understanding arsenate reaction kinetics with ferric hydroxides, *Environ. Sci. Technol.* 47 (2013) 8342–8347.